DOI: 10.1002/adma.200501267

Field-Emission Behavior of a Carbon-Nanotube-Implanted Co Nanocomposite Fabricated from Pearl-Necklace-Structured Carbon Nanotube/Co Powders**

By *Seung I. Cha*, *Kyung T. Kim*, *Salman N. Arshad*, *Chan B. Mo*, *Kyong H. Lee*, and *Soon H. Hong**

One of the most promising characteristics of carbon nanotubes (CNTs) is their outstanding field-emission behavior, especially their low-threshold electric fields and large emission-current densities.[1–4] Many research groups have developed various types of CNT emitters using the deposition of CNTs[5–8] and the screen-printing of CNT pastes.[9–13] However, there remain some critical technological challenges to the fabrication of large-area cold cathodes with long lifetimes and improved performance. In this study, we have fabricated pearl-necklace-structured CNT/Co powders in which Co nanoparticles are threaded by CNTs. These powders have been screen-printed and sintered to produce a CNT-implanted Co nanocomposite emitter, wherein one end of the CNT is implanted within the sintered Co layer and the other end is exposed to the free surface. During the sintering process, the CNTs straighten out and become aligned perpendicular to the substrate. The CNT-implanted Co nanocomposite emitter exhibits characteristic field-emission properties, including a relatively high current density. In addition, because of its characteristic morphology, the nanocomposite can be readily patterned on substrates with good adhesion, and thus it is expected that these materials can be readily used to fabricate large-area cold cathodes.

Since the first discovery of the excellent field-emission properties of CNTs,[1,2] there has been a great deal of research focused on developing CNT-based field-emission devices.[3–13] CNTs have a relatively low threshold voltage and high current density due to their high electrical conductivity, high aspect ratio, and sharp tip morphology.[3,4] However, CNTs deposited on substrates and metal electrodes using arc discharge or chemical vapor deposition do not perform well as field emitters, and are considered inadequate for large-area-display applications.[5–8] Although researchers have proposed printing CNT pastes consisting of CNTs and organic binders for large-area displays, critical problems remain, including low electrical conductivity and weak adhesion between screen-printed CNTs and metal electrodes.[9–12] In order to overcome these problems, some groups have proposed using a CNT/metal paste for screen printing, with the resultant paste consisting of CNTs, metal powders, and organic binders.[13] However, after screen printing a CNT/metal paste, the CNTs tend to agglomerate and are buried within the metal powders, necessitating further post-treatment and removal of the metal layer to expose the CNTs. Although the CNTs are exposed to the surface by post-treatment, they are simply embedded in the metal powder without any sort of alignment. In addition, the CNTs lying in the metal powder prevent the sintering of the powders into a continuous metal layer;[14] thus, the metal layer is unable to strongly grasp the CNTs, and, as a result, a good electrically conducting path cannot be established. At the same time, this discontinuous metal layer is difficult to pattern by etching. Therefore, the simple mixing of CNTs with metal powders does not solve critical issues, such as strong adhesion, high electrical conductivity, and good reliability. In order to overcome the above-mentioned problems and for efficient electron emission, perpendicularly aligned CNTs need to be implanted within a continuous metal layer while being simultaneously exposed to the surface.

In this study, we have fabricated a novel CNT-implanted Co nanocomposite emitter from pearl-necklace-structured CNT/Co powders, in which Co nanoparticles are threaded by penetrating CNTs, using a sintering process to cause CNTs to align perpendicularly on the substrate.

The key technology used for fabricating the pearl-necklace-structured CNT/Co powders involves attaching Co atoms to the CNT surfaces in a controlled way by homogeneously dispersing the nanotubes in a solvent, as shown in Figure 1. In the first step, multiwalled CNTs are homogeneously dispersed in dioctyl ether, which acts as a solvent for dispersing CNTs, as shown in Figure 1a. In the past, CNT functionalization has been a popular technique for dispersing CNTs to obtain CNT-implanted metal powders.[14] In order to protect CNTs from damage caused by the chemical reactions used to synthesize Co nanoparticles, oleylamine is used as a surfactant to disperse the CNTs. In the second step, cobalt acetylacetonate and 1,2-hexadecanediol are mixed with the CNT suspension, and the mixture is heated to the refluxing temperature of the solvent, causing Co nanoparticles to form on the CNT

[*] Prof. S. H. Hong, Dr. S. I. Cha, K. T. Kim, S. N. Arshad, C. B. Mo, K. H. Lee
Department of Materials Science and Engineering
Korea Advanced Institute of Science and Technology
373-1 Kusung-Dong Yusung-Gu, Daejeon 305-701 (Korea)
E-mail: shhong@kaist.ac.kr

[**] This research was supported by a grant (code No. 05K1501-00510) from the "Center for Nanostructured Materials Technology" under the "21st Century Frontier R&D Programs" of the Ministry of Science and Technology, Korea. Supporting Information is available online from Wiley InterScience or from the author.

ADVANCED MATERIALS

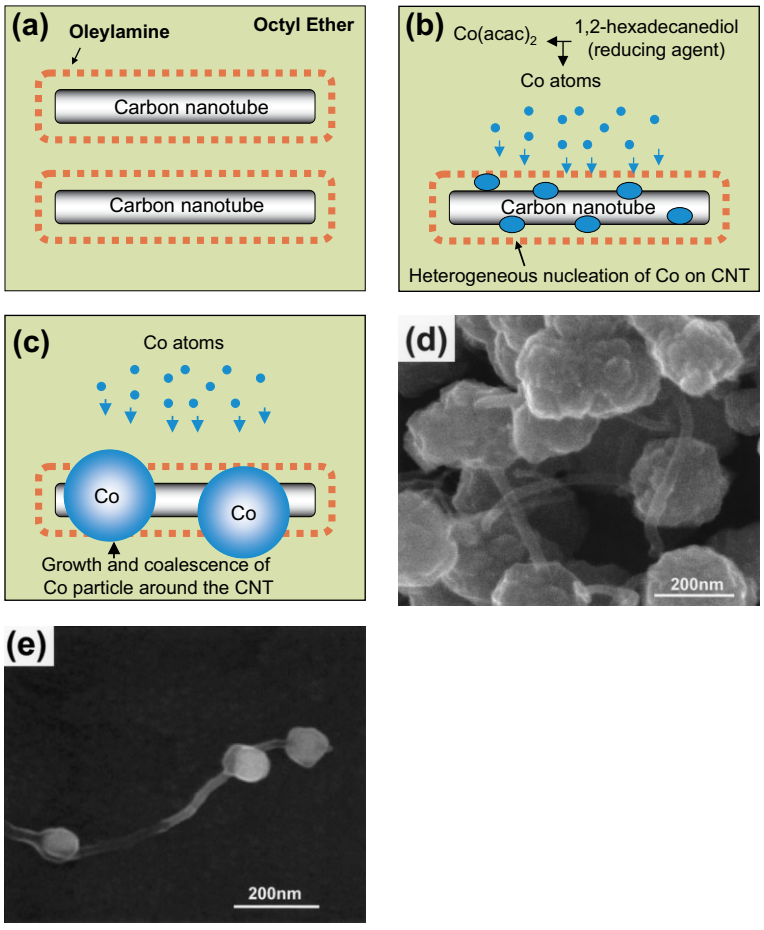

Figure 1. Schematic representation of the fabrication of pearl-necklace-structured CNT/Co powders: a) dispersion of CNTs in a solvent (dioctyl ether) with a surfactant (oleylamine); b) polyol process and heterogeneous nucleation of Co nuclei on dispersed CNTs; acac: acetylacetonate; and c) growth and coalescence of Co nuclei to form pearl-necklace-structured CNT/Co powders. d,e) Scanning electron microscopy (SEM) images of pearl-necklace-structured CNT/Co powders.

surfaces via a polyol process.[15,16] The CNTs dispersed homogenously in the solvent provide preferential nucleation sites for the heterogeneous nucleation of Co atoms, leading to the deposition of Co particles on the surfaces of the CNTs, as shown in Figure 1b. The Co nuclei on the CNT surfaces grow and coalesce to form pearl-necklace-structured CNT/Co powders, as shown in Figure 1c. In these powders, the Co nanoparticles are threaded by penetrated CNTs, as shown in Figure 1d.

The morphology of a CNT/metal powder depends on the interfacial energy between the metal and CNTs during the growth of the metal on the CNT surface. If the surface energy of CNTs, γ_{CNT}, is smaller than the interfacial energy between the metal and CNTs, $\gamma_{metal-CNT}$, as is the case for CNT/Cu, metal nanoparticles will not grow on CNTs (see Supporting Information). However, when γ_{CNT} is larger than $\gamma_{metal-CNT}$, such as for CNT/Ni, metal atoms tend to be located on the CNT surfaces, causing them to be coated with a metal layer (see Supporting Information). When γ_{CNT} is similar to $\gamma_{metal-CNT}$, as is the case for CNT/Co, metal atoms tend to be located on both CNTs and the metal. In this case, the metal particles take on a spherical shape and are threaded by CNTs, resulting in the pearl-necklace-structured CNT/Co powders shown in Figure 1d and Figure 2a.

Transmission electron microscopy (TEM) images of pearl-necklace-structured CNT/Co powders clearly show this morphology. Figure 2a shows spherical Co nanoparticles threaded by a CNT. The spherical particles have been identified as polycrystalline Co nanoparticles using high-resolution transmission electron microscopy (HRTEM), electron diffraction (Fig. 2b), and energy dispersive X-ray (EDX) analysis (Fig. 2c). The polycrystalline nature of the Co nanoparticles indicates that the Co nanoparticles are formed via a coalescence process during the growth of the Co nuclei. This is also supported by the fact that the average size of Co nanoparticles in the pearl-necklace-structured CNT/Co powder is about 93 nm, while Co nanoparticles fabricated using the same process, but without CNTs, have an average size of 65 nm, as shown in the particle-size distribution plot of Figure 2d.

The CNT-implanted Co nanocomposite emitter is fabricated from pearl-necklace-structured CNT/Co powders by a screen-printing process on indium tin oxide (ITO) glass followed by a sintering process, as shown in Figure 3a (see Experimental section for a detailed description of the process). Before sintering, the pearl-necklace-structured CNT/Co powders on ITO glass are buried in organic binders, which are thermally decomposed during the sintering process, as shown in Figure 3b. Thermogravimetric analysis (TGA) shows that the organic binder had been completely removed after the sintering process (see Supporting Information). During the sintering process, the Co nanoparticles climb down the CNTs and are sintered at the CNT base to form a dense metal layer in which the CNTs are implanted, as shown in Figure 3c. CNTs threaded into Co nanoparticles are simultaneously straightened and aligned perpendicular to the substrate so that they stand upright on the surface. The straightening of the CNTs is caused by the removal of CNT surface defects; previous sintering experiments under Ar caused CNTs of various shapes to revert to a defect-free state.[17] In addition, the CNTs tend to be aligned perpendicular to the substrate because the base of the nanotubes is implanted in the Co metal layer during the straightening process. This upright CNT behavior, along with the sintering of Co nanoparticles, is responsible for the characteristic microstructure of the CNT-implanted Co nanocomposite emitter, comprising CNT bases implanted in the sintered Co layer with the top parts of the CNTs exposed to the free surface, as shown in Figure 3d.

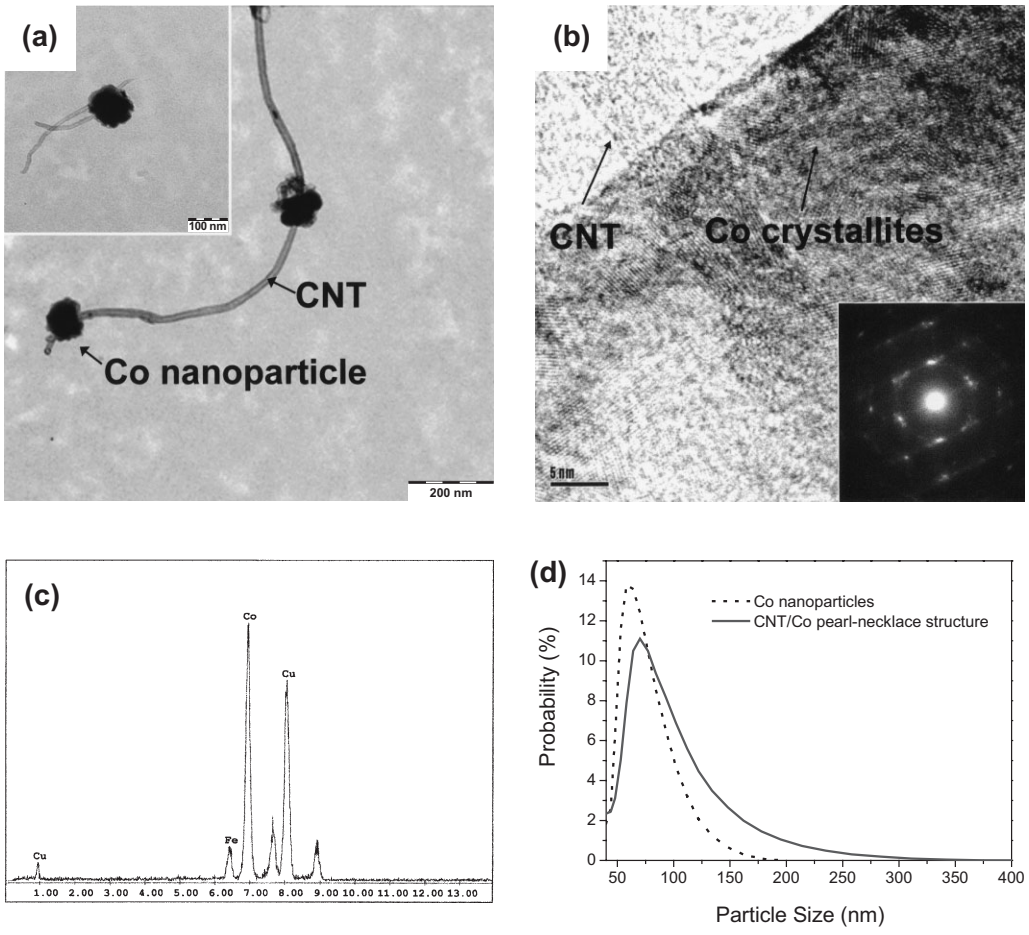

Figure 2. a) Transmission electron microscopy (TEM) images; b) high-resolution TEM (HRTEM) image and electron diffraction pattern; and c) TEM–energy dispersive X-ray analysis of pearl-necklace-structured CNT/Co powders. The Cu and Fe peaks originate from the TEM grid. d) Plot of the size distribution of Co nanoparticles in pearl-necklace-structured CNT/Co powders and in Co powders fabricated without CNTs.

The field-emission properties of CNT-implanted Co nanocomposite emitters have been measured at room temperature using a diode structure in a high-vacuum chamber. Figure 4a shows a typical plot of the emission current density versus the electric field applied between the cathode and anode in the diode structure. The turn-on field is 1.8 V μm^{-1} at an emission current density of 10 μA cm^{-1};[2,18] the maximum emission current density is 38–40 mA cm^{-2} at an electric field of 3.25 V μm^{-1}, which is comparable to that of carbon nanobells, which produce a current density of 200 mA cm^{-2} at 6 V μm^{-1}.[19] The CNT-implanted Co emitter has a lower turn-on field than screen-printed single-walled CNT emitters, which have been reported to have turn-on fields ranging from 2.2 to 4.2 V μm^{-1},[4,10–13,20–23] although we have used multiwalled CNTs as the emitters in this study. In addition, the current density of CNT-implanted Co nanocomposite emitters is 5–10 times higher than previously tested CNT emitters produced using single-walled CNT/metal or CNT pastes.[4,10–13,20–23]

The high current density of the CNT-implanted Co emitters is likely to be based on several factors. One probable factor is the low electrical resistance between the CNTs and the electrodes due to the characteristic morphology of these structures. The effect of the electrical resistance of the field emitter on field-emission behavior needs to be investigated further. Fowler and Nordheim proposed a relationship between the emission current and the electric field.[4] During the operation of field-emission devices, some fraction of the voltage is applied across the intrinsic emitter resistance. Thus, the applied voltage can be divided into two components: the first component involves field emission from the emitter, V_f, and the other portion is the voltage across the intrinsic electrical resistance of the emitter, V_0, as shown in Figure 4c. V_0 is directly proportional to the current and intrinsic electrical resistance, R. Therefore, the relationship proposed by Fowler and Nordheim[4] can be modified to relate the applied voltage, emission current, and intrinsic resistance

$$I = A[\beta(V - IR)]^2 \phi^{-1} \exp[-B\phi^{3/2}/\beta(V - IR)] \quad (1)$$

where I is the current, A and B are constants, ϕ is the work function of the emitter material, V is the applied voltage, and

ADVANCED MATERIALS

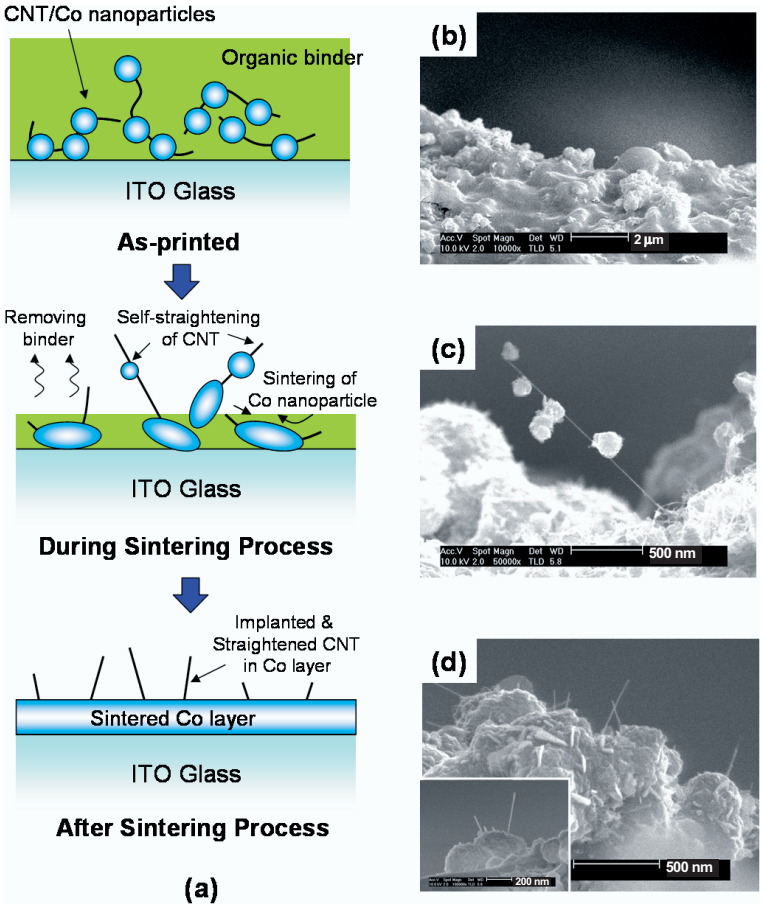

Figure 3. a) Schematic depiction of the fabrication process and formation mechanism for CNT-implanted Co nanocomposite emitters. b) Cross-sectional SEM image of screen-printed pearl-necklace-structured CNT/Co powders with an organic binder; c) SEM image showing Co nanoparticles threaded by a straight CNT after sintering at 400 °C; and d) SEM images of the CNT-implanted Co nanocomposite emitter after sintering at 400 °C.

β represents a shape factor. According to this equation, when the applied voltage is low, the intrinsic emitter resistance has only a small effect. As the applied voltage increases, the electric current is severely affected by the intrinsic resistance, as shown in Figure 4d. Analysis based on the intrinsic resistance in Equation 1 shows that the linear relationship in the Fowler–Nordheim plot is not maintained at high voltages, as shown in Figure 4e. This suggests that one possible reason for the nonlinearity in Fowler–Nordheim plots, reported in several studies of CNT emitters,[10,13] is the high electrical resistance of the field emitter. In addition, the intrinsic electrical resistance leads to nonlinearity in the Fowler–Nordheim plot with decreasing emission current. The origin of the intrinsic resistance seems to be interfacial resistance between the metal electrodes and the CNTs, because both the metal electrodes and the CNTs have high electrical conductivities. It is expected that a CNT-implanted Co nanocomposite emitter has a much lower intrinsic resistance at the interface between the metal electrodes and the CNTs than devices fabricated by screen-printing a CNT/metal or CNT paste.[10–13] This assumption is based on the characteristic structure of the CNT-implanted Co nanocomposite emitters. CNTs implanted in the Co layer lead to a sound interface and a large contact area between the CNTs and the metal electrodes; this is not achieved by the other processes.

A prototype field-emission display device based on the CNT-implanted Co nanocomposite, fabricated from pearl-necklace-structured CNT/Co powders by screen-printing followed by a sintering process, shows a uniform 1 cm^2 area of illumination, as shown in the Supporting Information. Another advantage of using a CNT-implanted Co nanocomposite emitter is that the CNT density within the emitter can be controlled to obtain the highest possible field-emission current density without shielding effects,[24,25] which are caused by excessively narrow spacing between CNTs.

In summary, pearl-necklace-structured CNT/Co powders, in which spherical Co nanoparticles are threaded onto penetrating CNTs, have been fabricated using a polyol-based process. These powders are screen-printed and sintered to produce a CNT-implanted Co nanocomposite emitter. During the sintering process, the Co nanoparticles climb down the CNTs and gather at the base. These particles are sintered together to form a dense Co layer with the CNTs implanted perpendicular to the substrate, thereby standing upright on the surface. The CNT-implanted Co nanocomposite emitters exhibit a low turn-on electric field and produce a high current density due to the low electrical resistance between the CNTs and the metal electrodes.

Experimental

Fabrication of CNT/Metal Nanoparticles: Cobalt(II) acetylacetonate ($Co(acac)_2$) was used as the Co metal source. Dioctyl ether was used as the solvent, oleylamine as a surfactant, and 1,2-hexadecanediol as the reducing agent. Iljin Nanotech (Korea) provided 0.3 mg of multi-walled CNTs. Oleylamine (0.125 mmol) was added to the solvent (10 mL dioctyl ether) in a 250 mL flask, and the mixture was stirred mechanically. The metal source (0.25 mmol) was added to the mixture, and 0.75 mmol of 1,2-hexadecanediol was added as a reducing agent. This mixture was sealed in an Ar atmosphere and refluxed for 2 h at 300 °C. After slowly cooling to room temperature, the CNT-implanted metal nanoparticles were washed with ethanol and hexane and separated by centrifugation at 10 000 rpm for 10 min, followed subsequently by drying under vacuum at 80 °C. The particle size distribution of the CNT-implanted Co nanoparticles was determined using a Beckman Coulter LS230 particle-size analyzer.

Fabrication and Characterization of CNT-Implanted Co Emitters: In order to fabricate a CNT-implanted Co cathode, CNT-implanted metal nanoparticles were mixed with an organic binder and screen-printed on 0.4 mm thick ITO glass. This screen-printed cathode was dried at 100 °C and sintered for 2 h at 400 °C in an Ar atmosphere.

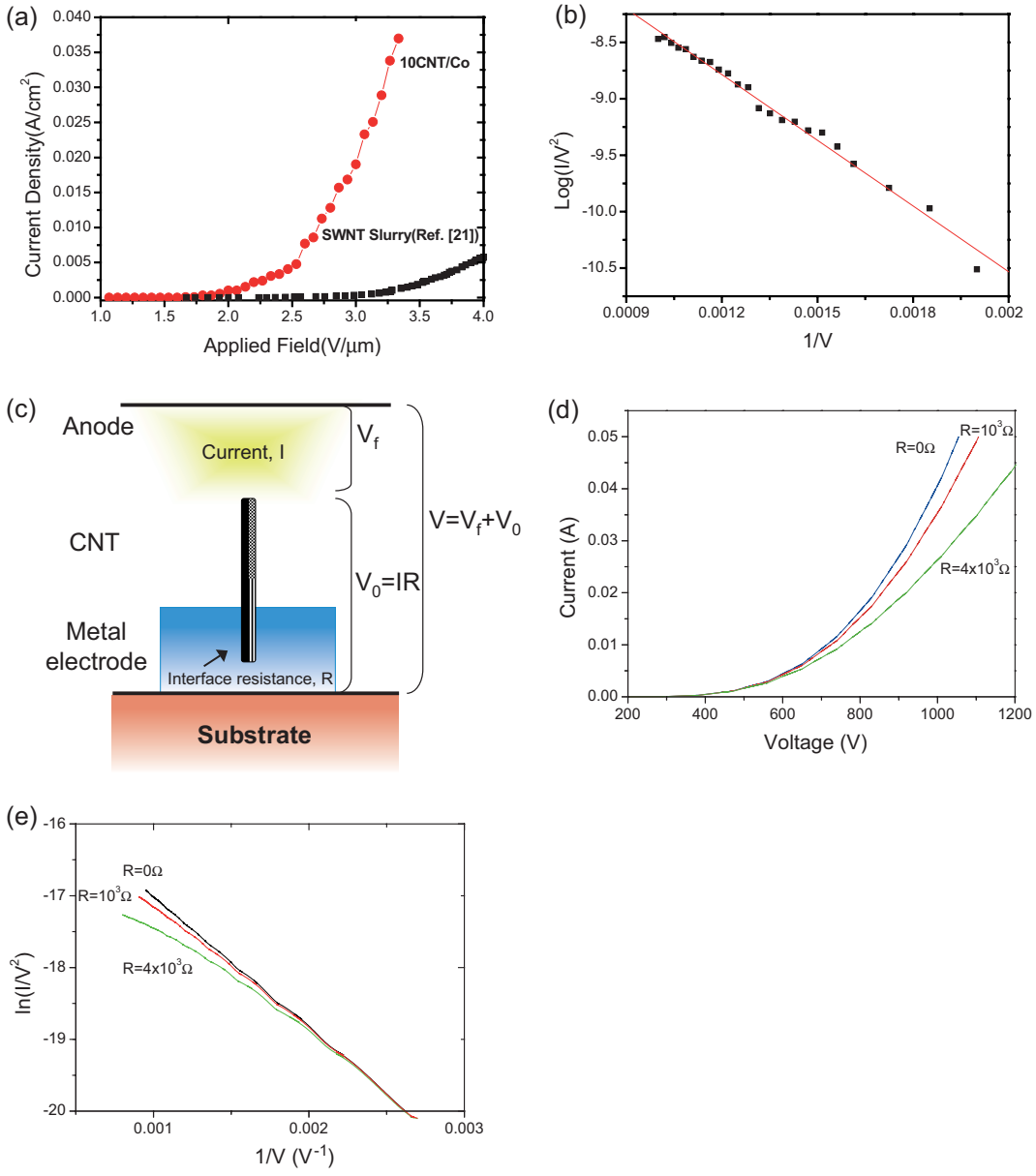

Figure 4. a) Plot of the applied electric field versus the emission current density and the Fowler–Nordheim plot (b) for a screen-printed CNT-implanted Co nanocomposite emitter prepared from pearl-necklace-structured CNT/Co powder by screen printing and sintering. The field-emission properties previously reported for a single-walled nanotube slurry are shown for comparison [21]); c) Schematic depiction of the diode-type field-emission device and the voltage applied to each part; d) the calculated relationship between the applied voltage (*V*) and the emission current (*I*) according to the intrinsic resistance model; and e) the Fowler–Nordheim plot of voltage and emission current according to the intrinsic resistance calculated in (d).

The field emission was measured in a high-vacuum chamber with a base pressure of 10^{-7} torr (1 torr ~ 133 Pa). Green phosphor-coated ITO glass was used as the anode. The distance between the cathode and anode was maintained at 300 μm, and a voltage of up to 1000 V was applied to the cathode to determine the field-emission properties.

Received: June 21, 2005
Final version: September 22, 2005

[1] A. G. Rinzler, R. E. Smalley, *Science* **1995**, *269*, 1550.
[2] W. A. de Heer, D. Ugarte, *Science* **1995**, *270*, 1179.
[3] R. H. Baughman, A. A. Zakhidov, W. A. de Heer, *Science* **2002**, *297*, 787.
[4] J. Bonard, M. Croci, C. Klink, R. Kurt, O. Noury, N. Weiss, *Carbon* **2002**, *40*, 1715.
[5] Y. Saito, Y. Nishina, *Nature* **1997**, *389*, 554.
[6] J. Bonard, J. Salvetat, T. Stockli, W. A. de Heer, L. Forro, A. Chatelain, *Appl. Phys. Lett.* **1998**, *73*, 918.
[7] S. Fan, A. M. Cassel, H. Dai, *Science* **1999**, *283*, 512.
[8] C. Bower, S. Jin, *Appl. Phys. Lett.* **2000**, *77*, 2767.
[9] Q. H. Wang, R. P. H. Chang, *Appl. Phys. Lett.* **1997**, *70*, 3308.
[10] Y. D. Kim, W. B. Choi, H. Wakimoto, S. Usami, H. Tomokage, T. Ando, *Appl. Phys. Lett.* **1999**, *75*, 3129.
[11] D. S. Chung, J. M. Kim, H. Wakimoto, S. Usami, H. Tomokage, T. Ando, *Appl. Phys. Lett.* **2002**, *80*, 4045.

[12] J. M. Kim, W. B. Choi, N. S. Lee, J. E. Jung, *Diamond Relat. Mater.* **2000**, *9*, 1184.
[13] D. S. Chung, W. B. Choi, J. H. Kang, H. Y. Kim, I. T. Han, Y. S. Park, Y. H. Lee, N. S. Lee, J. E. Jung, J. M. Kim, *J. Vac. Sci. Technol., B: Microelectron. Nanometer Struct.—Process., Meas., Phenom.* **2000**, *18*, 1054.
[14] S. I. Cha, K. T. Kim, S. N. Arshad, C. B. Mo, S. H. Hong, *Adv. Mater.* **2005**, *17*, 1377.
[15] *Encyclopedia of Nanoscience and Nanotechnology* (Ed: H. S. Nalwa), Vol. 1, American Scientific, Stevenson Ranch, CA **2004**, pp. 822–823.
[16] L. K. Kurihara, P. E. Schoen, *Nanostruct. Mater.* **1995**, *5*, 607.
[17] A. Hirsch, *Angew. Chem. Int. Ed.* **2002**, *41*, 1853.
[18] J. Hu, D. Golberg, *Adv. Mater.* **2004**, *16*, 153.
[19] X. Ma, E. Wang, W. Zhou, D. A. Jefferson, J. Chen, S. Deng, N. Xu, J. Yuan, *Appl. Phys. Lett.* **1999**, *75*, 3105.
[20] Y. R. Cho, K. I. Cho, *Jpn. J. Appl. Phys., Part 1* **2002**, *41*, 1532.
[21] B. Gao, O. Zhou, *Adv. Mater.* **2001**, *13*, 1770.
[22] J. Bonard, A. Chatelain, *Adv. Mater.* **2001**, *13*, 184.
[23] R. Collazo, R. Schlesser, Z. Sitar, *Appl. Phys. Lett.* **2001**, *78*, 2058.
[24] K. B. K. Teo, W. I. Milne, *Appl. Phys. Lett.* **2002**, *80*, 2011.
[25] J. S. Suh, J. S. Lee, *Appl. Phys. Lett.* **2002**, *80*, 2392.

